

Role of surface states in STM spectroscopy of (111) metal surfaces with Kondo adsorbates

J. Merino

*Departamento de Física Teórica de la Materia Condensada,
Universidad Autónoma de Madrid, Madrid 28049, Spain*

O. Gunnarsson

*Max-Planck-Institut für Festkörperforschung D-70506 Stuttgart, Germany
(Dated: August 20, 2018)*

A nearly-free-electron (NFE) model to describe STM spectroscopy of (111) metal surfaces with Kondo impurities is presented. Surface states are found to play an important role giving a larger contribution to the conductance in the case of Cu(111) and Au(111) than Ag(111) surfaces. This difference arises from the farther extension of the Ag(111) surface state into the substrate. The different line shapes observed when Co is adsorbed on different substrates can be explained from the position of the surface band onset relative to the Fermi energy. The lateral dependence of the line shape amplitude is found to be bulk-like for $R_{||} \lesssim 4 \text{ \AA}$ and surface-like at larger distances, in agreement with experimental data.

PACS numbers:

When a magnetic impurity is inside a metallic host, the Kondo effect can occur [1]. Signatures of the Kondo effect also appear in STM measurements of noble metal surfaces with adsorbed Kondo impurities through the appearance of characteristic zero bias line shapes [2, 3] of the Fano-type [4]. These line shapes are found to depend strongly on the metal surface on which the magnetic atom is adsorbed. For instance, the line shape associated with Co on Au(111) is more asymmetric than on Cu(111) whereas for Co on Ag(111) a rather symmetric line shape is observed. As both bulk and surface states are present in (111) surfaces it is yet an open question which of these play the most important role in the Kondo effect and what determines the line shapes observed for the different substrates.

In spite of the large amount of experimental work dedicated to the characterization of line shapes associated with different noble metal surfaces a complete theoretical model for the tip-surface-adsorbate interaction is yet lacking. The interaction of bulk states in the metal with the tip and adsorbate has been done through a Jellium model for the surface with step [5, 6], image [7] and Jones, Jennings and Jepsen (JJJ) [8] potentials. Tight-binding approaches have also been introduced [9]. However, the contribution of surface states to the conductance has only been partially discussed [6, 7].

Previously, we studied the tip-substrate-adsorbate interaction considering bulk states only [10]. In this Letter, we introduce a NFE description of the substrate which is the simplest way to describe bulk and surface states on equal footing. Surface states are found to give a substantial contribution to the STM conductance even when the tip is right above the Kondo impurity. This contribution varies from surface to surface and is larger for Cu(111) and Au(111) than for Ag(111). This can be understood

from the fact that the surface state in Ag(111) extends far into the substrate. Finally we find that the position of the surface band onset relative to the Fermi energy, ϵ_F , determines the different line shapes observed in the different substrates.

A NFE description of the surface is introduced. The ionic potential in the (111) direction is taken into account as a perturbation to the Jellium potential inside the crystal. This potential opens up a gap and surface states split from the bulk band edges. Since the weight of the surface states is removed from the bulk states one might expect that they are not important for integrated properties. However, they can be relevant to Fermi energy properties such as the STM conductance. Apart from including surface states we make similar assumptions as in Ref. [10]: (i) we neglect the direct coupling of the tip with the substrate d bands and with the 3d orbital of the adsorbate due to the localized nature of the d orbitals [11] and the large tip-surface separation, (ii) the adsorbate is modelled by a single $d_{3z^2-r^2}$ -orbital and the tip by a single s-orbital [12, 13], and (iii) the momentum dependence (including orthogonalization effects) of the hybridization matrix elements are explicitly taken into account [10, 14].

When Co is deposited on a noble metal surface, it captures electronic charge so that there is effectively only one hole left [15]. The unpaired spin residing in Co is responsible for the Kondo effect experimentally observed. Hence, we introduce a generalized Anderson model to describe the substrate, adsorbate and the tip. Neglecting the orbital degeneracy of the 3d orbital the model reads

$$H = \sum_{\mathbf{k},\sigma} \epsilon_{\mathbf{k}} c_{\mathbf{k}\sigma}^\dagger c_{\mathbf{k}\sigma} + \epsilon_d \sum_{\sigma} d_{\sigma}^\dagger d_{\sigma} + \sum_{\mathbf{k},\sigma} V_{\mathbf{k}} (d_{\sigma}^\dagger c_{\mathbf{k}\sigma} + H.c.) + U d_{\uparrow}^\dagger d_{\downarrow} d_{\uparrow} d_{\downarrow}$$

$$+ \sum_{\mathbf{k}, \sigma} M_{\tilde{\mathbf{k}}} (c_{\mathbf{k}\sigma}^\dagger t_\sigma + H.c.) + H_t. \quad (1)$$

Here, ϵ_d is the energy level of the adsorbate d orbital, $c_{\mathbf{k}\sigma}^\dagger$ creates an electron with spin σ and momentum $\tilde{\mathbf{k}}$. $d_{\tilde{\mathbf{k}}}^\dagger$ and t_σ^\dagger create an electron in the $d_{3z^2-r^2}$ orbital of the adsorbate and the s -orbital of the tip, respectively. $\epsilon_{\tilde{\mathbf{k}}}$ and $V_{\tilde{\mathbf{k}}}$ are the metallic energies and the hybridization matrix elements between the substrate and the adsorbate, respectively. U is the Coulomb repulsion of two electrons in the adsorbate. The last two terms in the model are the tip-substrate interaction which is governed by the matrix elements, $M_{\tilde{\mathbf{k}}}$, and H_t that describes the tip which is supposed to have an unstructured density of states.

The modification of the STM conductance through the surface due to the presence of the 3d impurity is given by [10]

$$\delta G(\omega) = G_0 \rho_t \text{Im} \{ (A(\omega) + iB(\omega)) G_{dd}(\omega) (A^*(\omega) + iB^*(\omega)) \}, \quad (2)$$

with $G_0 = \frac{4e^2}{h}$ and ρ_t the tip density of states.

In the above equation, $B(\omega)$, reads

$$B(\omega) = \pi \sum_{\mathbf{k}} M_{\tilde{\mathbf{k}}} V_{\tilde{\mathbf{k}}} \delta(\omega - \epsilon_{\mathbf{k}}) + \pi \sum_{\mathbf{k}_{||}} M_{\tilde{\mathbf{k}}_{||}} V_{\tilde{\mathbf{k}}_{||}} \delta(\omega - \epsilon_{\mathbf{k}_{||}}), \quad (3)$$

where a sum over the two bulk bands appearing due to the ionic potential in the (111)-direction is understood in the \mathbf{k} sum.

The first term in Eq. (3) describes the interaction of the adsorbate and tip with bulk states and the second describes the interaction with the surface band. $A(\omega)$ is the Kramers-Kronig transformation of $B(\omega)$. Matrix elements, $M_{\tilde{\mathbf{k}}}$ and $V_{\tilde{\mathbf{k}}}$, are evaluated with the orthogonalized wavefunctions, $|\tilde{\mathbf{k}}\rangle$. Details are given in Ref. [10]. For the systems of interest here, $A(\omega)$ and $B(\omega)$ are real. The crucial quantity is $B(\omega)$ as it embodies the complete information concerning the tip-substrate-adsorbate system. $B(\omega)$ depends on the tip position, $\mathbf{R} = (\mathbf{R}_{||}, Z_t)$, the adsorbate position, $(0, Z_d)$, where Z is referred to the last plane of ions. The metal potential, V_M , comes in the matrix elements, $V_{\tilde{\mathbf{k}}}$ and $M_{\tilde{\mathbf{k}}}$. We define throughout the paper $R_{||} = |\mathbf{R}_{||}|$. The Green's function, $G_{dd}(\omega)$, describes the electronic properties of the 3d adsorbate immersed in the metallic continuum including many-body effects such as the Kondo effect. The Kondo peak is simulated through a Lorentzian of width T_K positioned at ϵ_K and is contained in $G_{dd}(\omega)$ with T_K and ϵ_K taken from experimental data. These parameters vary between $\epsilon_K \sim 3 - 6$ meV and $T_K \sim 50 - 90$ K for the different (111) surfaces [2, 16, 17].

Metal wavefunctions are obtained by solving Schrödinger's equation in the presence of the surface potential, which is given (in Rydberg energy units)

TABLE I: Surface state data and parameters used in a NFE model of (111) noble metal surfaces. The depth of the crystal potential, V_0 , the first Fourier component of the ion potential, V_G , and the metal work function, W , are taken from Ref. [18] and are given in eV's. V_0 is referred to the vacuum level while the surface state energy is referred to the Fermi energy, ϵ_F . The lattice parameter, a , and the decay of the surface state into the bulk, λ_{ss} , are given in Å while the steepness of the potential denoted as λ , is given in Å⁻¹.

Surface	a	V_0	V_G	W	λ	Z_{im}	$\epsilon_{ss} - \epsilon_F$	m_{ss}/m_e	λ_{ss}
Cu(111)	3.64	14.7	2.55	4.95	2.21	1.29	-0.32	0.38	10.4
Ag(111)	4.08	15.1	2.1	4.74	2.23	1.28	-0.05	0.39	28.6
Au(111)	4.07	17	2.3	5.30	2.36	1.25	-0.49	0.26	13.5

by:

$$V_M(Z) = \begin{cases} \frac{-1}{2(Z-Z_{im})} (1 - e^{-\lambda(Z-Z_{im})}) & , Z > Z_{im} \\ \frac{-V_0}{Ae^{\beta(Z-Z_{im})} + 1} & , Z_m < Z < Z_{im} \\ -V_0 + 2V_G \cos(GZ) & , Z < Z_m \end{cases} \quad (4)$$

where Z is the perpendicular direction to the surface (the (111) direction). V_0 is the depth of the bulk potential and λ controls the sharpness of the surface barrier potential. The parameters $A = 2V_0/\lambda - 1$ and $\beta = V_0/A$ are obtained by imposing the condition of continuous differentiability of the JJJ potential at $Z = Z_{im}$ (see Ref. [8] for more details). Z_m is obtained by matching the periodic part of the potential in the perpendicular direction to the surface with the JJJ potential. All distances are referred to the last plane of ions and energies are referred to the vacuum level unless otherwise stated. G is the reciprocal vector along the perpendicular direction to the surface (the (111) direction) and V_G is the first Fourier component of the crystal potential associated with G . For the (111) surfaces $G = 2\pi\sqrt{3}/a$, where a is the lattice parameter.

The periodic part of the potential inside the crystal couples the $|\mathbf{k}\rangle$ and $|\mathbf{k} + \mathbf{G}\rangle$ states, leading to a gap of size: $E_G = 2|V_G|$. For perpendicular momenta: $0 \leq k_z \leq G/2$ and energies outside the gap, bulk wavefunctions are obtained by matching the wavefunctions outside and inside the crystal. Wavefunctions are free electron-like far from the band edges but differ from this description close to them.

Surface states are possible inside the gap with momentum $k_z = G/2 + i/\lambda_{ss}$. These states decay inside the bulk with the decay length, λ_{ss} , retaining the periodicity parallel to the surface. By matching the complex solution inside the bulk with the solution outside we solve for the energy at which the surface state exists [19].

Wavefunctions associated with these surface states

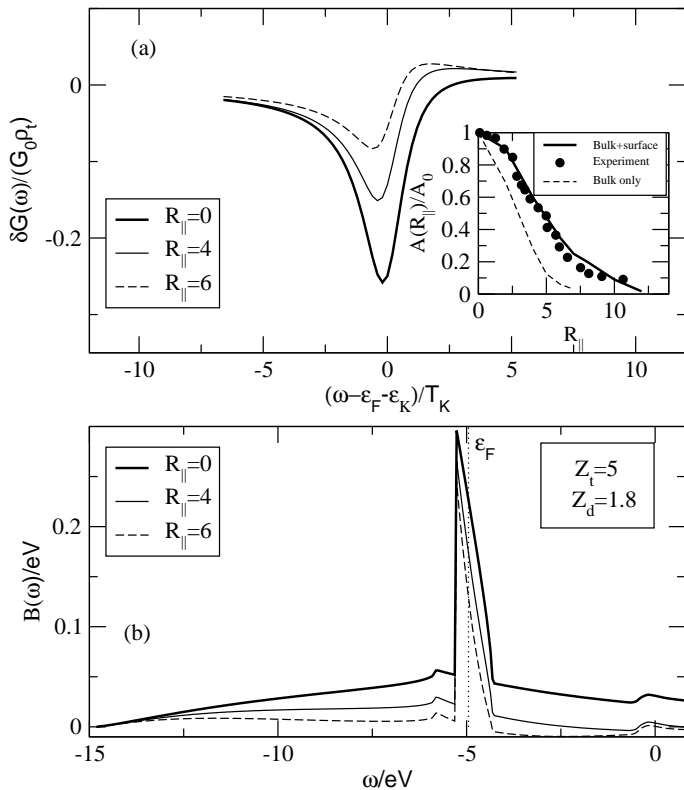


FIG. 1: Conductance line shapes obtained from the NFE model for Co on Cu(111). In (a) we show conductance line shapes for different lateral positions of the tip associated with the function $B(\omega)$ displayed in (b). The inset shows the lateral variation of the normalized conductance amplitude, $A(R_{||})/A_0$ compared to experimental data. Distances are given in \AA .

read

$$\Psi(\epsilon, \mathbf{r}) = \begin{cases} \frac{D}{\sqrt{\sigma}} e^{i\mathbf{k}_{||}\mathbf{r}_{||}} e^{(z-Z_m)/\lambda_{ss}} \cos\left(\frac{G}{2}z + \theta(\epsilon)\right) & , z < Z_m \\ e^{i\mathbf{k}_{||}\mathbf{r}_{||}} \psi(\epsilon, z) & , z > Z_m \end{cases} \quad (5)$$

where, $\psi(\epsilon, z)$, is the solution to the Schrödinger equation in the perpendicular direction for a given energy, ϵ . σ is the area of the square enclosing the surface wavefunction and $\theta(\epsilon)$ is the phase factor coming from the solution of Schrödinger's equation inside the bulk. Surface states with larger λ_{ss} penetrate more into the solid and correspond to surface state energies closer to the bulk band edge. The normalization constant, $D \sim \sqrt{1/\lambda_{ss}}$ for $\lambda_{ss} \gg 1$, going to zero as the surface state energy approaches the bulk continuum. This constant is important to determine the relative contribution of surface states compared to bulk states in the conductance.

The surface state energy is determined by keeping all parameters describing the surface potential fixed except for Z_{im} which is varied to recover the surface state po-

sition in agreement with photoemission data [18]. The values of Z_{im} obtained are shown in Table I. For instance, for Cu(111) a surface state at 0.32 eV appears below the Fermi energy and the first image state at 0.83 eV below the vacuum level for $Z_{im} = 1.29 \text{ \AA}$ in good agreement with experimental values. Bulk-band effective masses, $m^*/m_e = 0.74, 0.55,$ and 0.52 are taken in the (111) direction and $0.25, 0.36$ and 0.18 in the parallel direction for Cu, Ag and Au, respectively. In our calculations of $B(\omega)$ we neglect the image state band as it is far from the Fermi energy and disperses over a rather small energy range, leading to a small contribution to $A(\epsilon_F)$.

Parameters describing surface bands of Cu(111), Au(111) and Ag(111) surfaces are summarized in Table I, where relevant parameters of the surface potential together with values of λ_{ss} and surface band effective masses, m_{ss} , are displayed. These masses are in good agreement with available experimental data from STM of clean surfaces [16, 20, 21] and photoemission data [18].

The conductance for the three noble metal surfaces with Co adsorbed on them is calculated. Results for $B(\omega)$ and conductance line shapes are displayed in Fig. 1 to Fig. 3 for Cu, Au and Ag, respectively. Most of the contribution to $B(\omega)$ close to the Fermi energy comes from the surface band and is larger for Cu(111) and Au(111) than for Ag(111) as expected as in this case the surface state penetrates more into the crystal. At the same time $B(\omega)$ has a rapid drop with increasing ω . This is because as the surface band disperses it gradually approaches the bulk continuum so that at a certain energy the surface band hits the bulk band and its amplitude drops to zero.

Depending on the position of the surface band onset relative to the Fermi energy, the conductance line shape becomes more or less symmetric. If there is more weight below the Fermi energy, the conductance line shape is asymmetric with positive Fano parameter, $q > 0$ (see Fig. 1 of Ref.[10]). From Table. I we see that $|\epsilon_{ss} - \epsilon_F|$ is smallest for Ag(111) and largest for Au(111). Hence, the most asymmetric line shape corresponds to Au(111) and the most symmetric one to Ag(111). The different line shapes calculated for the different substrates are in agreement with experimental observations.

The conductance amplitude, $A(R_{||})$, is more rapidly suppressed at short distances $R_{||} \lesssim 4 \text{ \AA}$ than for $R_{||} > 4 \text{ \AA}$. This is because both bulk and surface states contribute to $B(\epsilon_F)$. As the tip is displaced laterally the bulk contribution to $B(\omega)$ close to ϵ_F drops quickly until it eventually vanishes. Farther apart from the impurity, the surface band dominates and the lateral dependence becomes surface-like. Had we considered bulk states only in our model, $A(R_{||} = 6)/A_0 \sim 3\%$, which is an order of magnitude smaller than the one found experimentally[17]. This is because $A(R_{||}) \sim 1/R_{||}^2$ for bulk states. In contrast, the amplitude dependence on $R_{||}$ is in good agreement with our calculations when both surface and bulk states are

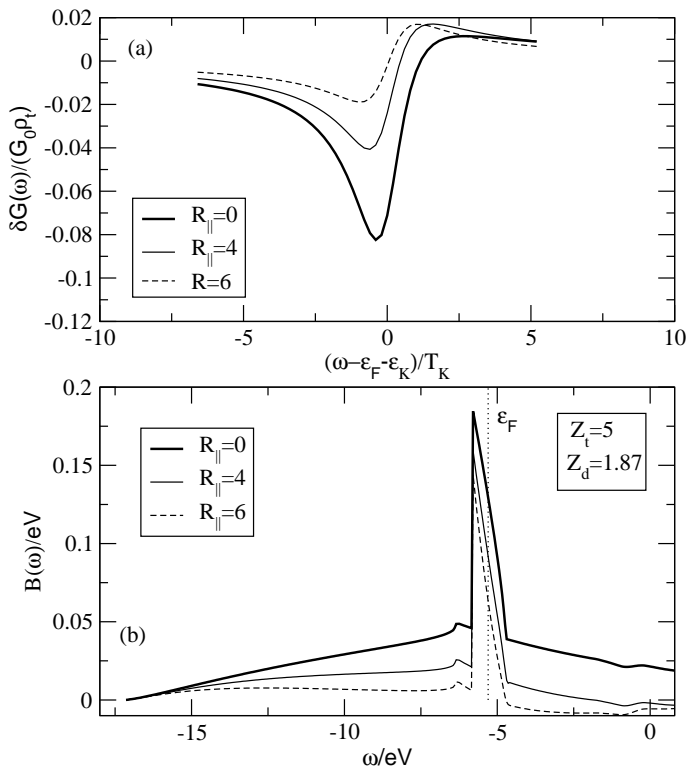


FIG. 2: Conductance line shapes calculated from the NFE model for Co on Au(111). Line shapes become more asymmetric with more positive Fano parameter as $\epsilon_F - \epsilon_{ss}$ increases (compare the plotted line shape for Au(111) with the ones shown in Figs. 1 and 3).

included (see inset of Fig. 1).

In conclusion, surface bands give an important contribution to the conductance in STM measurements of (111) noble metal surfaces with Kondo adsorbates. The position of the surface band onset relative to the Fermi energy determines the line shapes in the different (111) substrates. The lateral variation of the amplitude is found to be bulk-like close to the adsorbate becoming surface-like for $R_{\parallel} > 4 \text{ \AA}$ in agreement with experimental observations.

We acknowledge helpful discussions with Y. Dappe, P. Jelinek, M. A. Schneider and P. Wahl. M. A. S. and P. W. for lending their experimental data to us. J. M. acknowledges financial support from the Ramón y Cajal program from Ministerio de Ciencia y Tecnología in Spain.

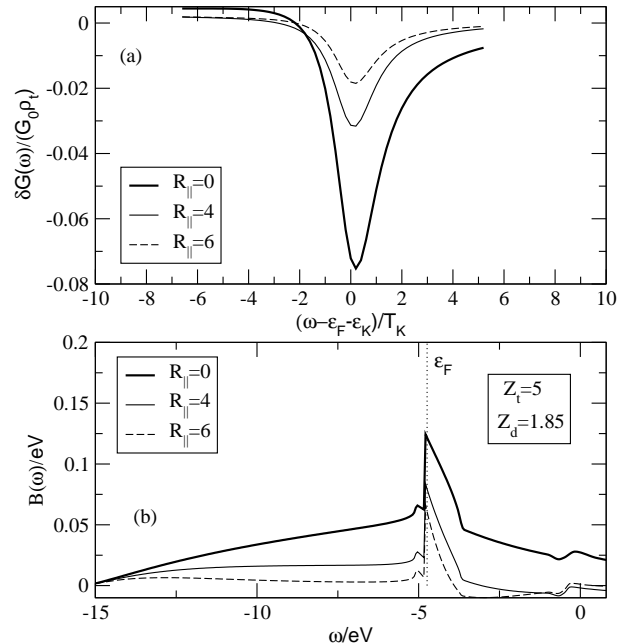


FIG. 3: Conductance line shapes calculated from the NFE model for Co on Ag(111). The surface band gives the smallest contribution of the three noble metal surfaces to $B(\omega)$ and the conductance.

[1] J. Kondo, Prog. Theor. Phys. (Kyoto), **32**, 39 (1964).
 [2] V. Madhavan, W. Chen, T. Jamneala, M. F. Crommie, N. S. Wingreen, Science **280**, 567 (1998).
 [3] J. Li, W-D Schneider, R. Berndt, and B. Delley, Phys. Rev. Lett. **80** 2893 (1998).

[4] U. Fano, Phys. Rev. **124**, 1866 (1961).
 [5] N. D. Lang, Phys. Rev. B **34** 5947 (1986).
 [6] M. Plihal and J. Gadzuk, Phys. Rev. B **63**, 085404 (2001).
 [7] C. Y. Lin, A. H. Castro-Neto, and B. A. Jones, cond-mat/0307185.
 [8] R. O. Jones, P. J. Jennings, and O. Jepsen, Phys. Rev. B **29** 6474 (1984).
 [9] A. Schiller and S. Hershfield, Phys. Rev. B **61**, 9036 (2000).
 [10] J. Merino and O. Gunnarsson, to appear in Phys. Rev. B.
 [11] V. Madhavan, W. Chen, T. Jamneala, M. F. Crommie, and N. S. Wingreen, Phys. Rev. B **64**, 165412 (2001).
 [12] J. Tersoff and D. R. Hamann, Phys. Rev. B **31**, 805 (1985).
 [13] J. Gadzuk, Phys. Rev. B **47**, 12832 (1993).
 [14] T. B. Grimley, *Electronic Structure and Reactivity of Metal Surfaces*, edited by E. G. Derouane and A. A. Lucas (Plenum Press, New York, 1976), p. 113.
 [15] O. Újsághy, J. Kroha, L. Szunyogh, and A. Zawadowski, Phys. Rev. Lett. **85** 2557 (2000).
 [16] M. A. Schneider, L. Vitali, N. Knorr, and K. Kern, Phys. Rev. B **65** 121406 (2003).
 [17] N. Knorr, M. A. Schneider, L. Diekhöner, P. Wahl, and K. Kern, Phys. Rev. Lett. **88**, 096804 (2002).
 [18] N. V. Smith, C. T. Chen, and M. Weinert, Phys. Rev. B **40** 7565 (1989).
 [19] N. V. Smith, Phys. Rev. B **32** 3549 (1985).
 [20] G. Fiete, *et. al.*, Phys. Rev. Lett. **86**, 2392 (2001).
 [21] W. Chen, V. Madhavan, T. Jamneala, and M. F. Crommie, Phys. Rev. Lett. **80**, 1469 (1998).